Possible persistence of fractional quantum Hall effect down to ultralow fillings

Michael R. Peterson and Jainendra K. Jain
Department of Physics, 104 Davey Laboratory, The Pennsylvania State University, University Park, Pennsylvania 16802, USA
(Received 5 June 2003; published 14 November 2003)

A recent theoretical study indicating that the fractional quantum Hall liquid is the ground state at $\nu=1/9$ is inconsistent with an excitonic instability of the fractional quantum Hall liquid found earlier at the same filling factor. This paper shows that, when the calculation is improved perturbatively, by allowing mixing between composite fermion Landau levels, the instability disappears. In fact, no instability occurs in our theory for filling factors as low as $\nu=1/31$, suggesting that the fractional quantum Hall effect may be robust down to much smaller filling factors than presently believed.

DOI: 10.1103/PhysRevB.68.195310 PACS number(s): 71.10.Pm, 73.43.−f

I. INTRODUCTION

It is believed that the fractional quantum Hall effect[1–3] (FQHE) liquid will undergo a phase transition into a Wigner crystal[4] (WC) state at sufficiently low values of the electronic Landau level (LL) filling factor ν. The phase transition had been previously thought[5–8] to occur at $\nu^{-1}\approx 6.5$, but the experimental evidence has been conflicting. On the one hand, the insulating state on both sides of $\nu=1/5$ and for filling factors below $\nu=1/5$ was interpreted in terms of a Wigner crystal.[9–11] On the other, experiments reported[12–14] evidence for a FQHE at $\nu=1/7$, 2/11, and 1/9, and recent investigations[15] in very high quality samples have indicated the presence of rather extensive FQHE at filling factors less than $\nu=1/6.5$, with evidence for $\nu=1/7$, 2/11, 2/13, 3/17, 3/19, 2/15, 2/17, and 1/9. This has led to renewed interest in the issue of where a quantum phase transition from the FQHE liquid to the Wigner crystal takes place.

In a recent paper,[16] we have improved upon the ground-state energy of the liquid within the composite fermion theory,[17] by allowing mixing between composite fermion Landau levels, which had been neglected previously. (It is stressed that our theory below will be confined strictly to the lowest *electronic* Landau level.) Although such mixing lowered the energy only by $<1\%$, that small energy change qualitatively affected the phase boundary between the FQHE liquid and the Wigner crystal. Comparisons with best available estimates for the energy of the WC (Refs. 5 and 6) showed that the ground state of the system is very likely the composite-fermion (CF) liquid for $\nu=1/7$ and 1/9, and quite possibly also at $\nu=1/11$.

This conclusion is inconsistent with an earlier calculation[18] which considered the excitation spectrum and found that for $\nu\leqslant 1/9$ the CF exciton had lower energy than the assumed ''ground state,'' thus signaling an instability of the FQHE liquid. The instability occurs, in that calculation, at a wave vector that is very close to the reciprocal-lattice vector of the Wigner crystal, consistent with the expected transition. It was noted that because the instability was found in a theory that used the same physics for the construction of the ground and the excited states, the result was presumably less sensitive to the accuracy of the trial wave functions than the comparisons between the FQHE and WC variational wave functions, which are based on different physical approaches.

In this paper, we revisit the issue of excitonic instability of the FQHE state, armed with the more sophisticated methods developed since Ref. 18. We investigate how the energy of the neutral CF exciton is modified by CF-Landau level mixing, caused by weak residual interaction between the composite fermions. As shown below, the energy of the uniform liquid is reduced substantially relative to the excitations at $\nu=1/9$, eliminating the instability found in Ref. 18. Self-consistency with the ground-state energy comparisons is thus achieved at the current level of accuracy.

This raises the question of when, ultimately, a transition from the CF liquid to the WC takes place. As explained in Ref. 16, an accurate determination of whether the CF liquid or the Wigner crystal is the ground state becomes more and more difficult as the filling factor is reduced, because of the very small energy difference between the two states, and because the thermodynamic extrapolation introduces additional uncertainties. On the other hand, the present method of considering excitations can be taken to much lower fillings. We find no instability down to $\nu=1/31$.

Even though our results are very accurate, certainly the best theoretical estimates presently available, the usual caveats of any variational study apply. While precise calculations for the energy differences between the ground and excited states can be performed for our model, it is difficult to judge, in general, how trustworthy the model itself is, especially when the energy differences are very small. Also, a first-order transition into a crystalline state can occur without the vanishing of an excitation energy, so the absence of the latter does not rule out a transition into a WC in the filling factor region considered here. For these reasons, the final answer to the question ''How low can the FQHE go?'' raised in the title will come only from experiment, but our study does suggest the possibility that the FQHE may be more robust and extend to smaller filling factors than earlier believed.

We note that it is entirely possible that at low fillings the actual state goes into a complex ''alternating phase,'' with the FQHE liquid at certain special filling factors and the Wigner crystal in between. There is already evidence[9–11] for such a re-entrant phase near $\nu=1/5$.

The neutral excitations are of relevance to a number of issues other than the liquid-solid transition considered here.

They have been measured directly in inelastic light scattering[19–22] and also via ballistic phonon scattering[23,24] for many filling factors of the type $\nu=n/(2n\pm1)$. Similar direct measurements are in principle possible at low fillings. The neutral excitations also govern several thermodynamic quantities, such as entropy and specific heat.

II. COMPOSITE FERMION THEORY

In this section, we briefly outline the features of the composite fermion theory used in our work as well as aspects of the specific geometry in which our calculation is performed.

In the composite fermion theory[17] of the FQHE, strongly interacting electrons capture an even number ($2p$, p integer) of quantized vortices to transform into weakly interacting composite fermions in order to most effectively minimize the Coulomb interaction energy. A composite fermion is often imagined as an electron bound to $2p$ magnetic flux quanta, where $\phi_0=hc/e$ is the elementary quantum of magnetic flux. A composite fermion consisting of $2p$ vortices attached to an electron is denoted by ^{2p}CF. The composite fermions experience a reduced magnetic field (due to the vortex binding), and have a filling factor ν^*, given by the relation $\nu=\nu^*/(2p\nu^*\pm1)$, where ν is the electron filling factor. When the composite fermions occupy an integral number (n) of CF Landau levels an energy gap appears resulting in the phenomenon of the FQHE. The fractional QHE of electrons at $\nu=n/(2pn\pm1)$ is thus a manifestation of the integral QHE of composite fermions at $\nu^*=n$. For example, a system with ^{8}CF's occupying one, two, or three CF LL's corresponds to the electron filling factors $\nu=1/9$, 2/17, or 3/25, respectively.

In the following, we will make use of the spherical geometry where N interacting electrons are placed on the surface of a sphere under the influence of a radial magnetic field produced by a magnetic monopole of strength Q at the center of the sphere. This is a convenient geometry when studying bulk properties of the system because of the absence of any boundaries. The flux through the sphere is equal to $2Q\phi_0$, where Q is an integer or a half integer according to the Dirac quantization condition. The single-particle eigenstates are the monopole harmonics[25] $Y_{Qnm}(\Omega_j)$. Here, $n=0,1,\ldots$ denotes the LL index, $m=-(Q+n),-(Q+n)+1,\ldots,Q+n$ labels the $2(Q+n)+1$ degenerate states in the nth LL, and $\Omega_j=(\theta_j,\phi_j)$ represents the location on the sphere of particle j with the usual spherical coordinates. Further, we assume that all the electrons are fully spin polarized, which is often the case at the very small filling factors of present interest due to the very strong magnetic fields required.

According to the CF theory, strongly interacting electrons at Q are mapped into weakly interacting composite fermions at the effective monopole strength $q=Q-p(N-1)$. The wave function for interacting electrons at Q is constructed as

$$\Psi=P_{LLL}\Phi_1^{2p}\Phi, \tag{1}$$

where Φ is the wave function for electrons at flux strength q, Φ_1 is the wave function of the lowest filled electronic LL:

$$\Phi_1^{2p}=\prod_{j<k}(u_jv_k-v_ju_k)^{2p}\exp[ip(\phi_j+\phi_k)], \tag{2}$$

where $u_j\equiv\cos(\theta_j/2)e^{-i\phi_j/2}$, $v_j\equiv\sin(\theta_j/2)e^{i\phi_j/2}$, and P_{LLL} is the lowest LL projection operator.

The zeroth-order approximation for the ground-state wave function at $\nu=n/(2pn+1)$ is obtained with Φ equal to the single Slater determinant of n filled Landau levels. In this case, because the wave function Ψ is obtained from noninteracting electrons at $\nu^*=n$, we will refer to it as the noninteracting composite fermion wave function at CF filling factor $\nu^*=n$ and denote it by $\Psi^{(0)}$. It ought to be stressed that noninteracting composite fermions provide a theory of strongly interacting electrons at electron filling factor $\nu=n/(2pn+1)$. Further, since $\Psi^{(0)}$ describes an integral number of completely filled CF LL's it is a filled shell state with total angular momentum $L=0$.

One of the important technical aspects of our calculation is the projection of the wave functions into the lowest electronic LL. It has been shown in Refs. 26 and 27 that after such a projection, we get

$$\Psi=\Phi^{CF}, \tag{3}$$

where Φ^{CF} has exactly the same form as Φ but with the single-particle eigenstates $Y_{qnm}(\Omega_j)$ in Φ replaced by "single-CF" particle eigenstates Y^{CF}_{qnm}, where

$$\begin{aligned}Y^{CF}_{qnm}(\Omega_j)=N_{qnm}(-1)^{q+n-m}\frac{(2Q+1)!}{(2Q+n+1)!}u_j^{q+m}v_j^{q-m}\\ \times\sum_{s=0}^{n}(-1)^s\binom{n}{s}\binom{2q+n}{q+n-m-s}\\ \times u_j^sv_j^{n-s}\left[\left(\frac{\partial}{\partial u_j}\right)^s\left(\frac{\partial}{\partial v_j}\right)^{n-s}J_j^p\right]\end{aligned} \tag{4}$$

with normalization factor

$$N_{qnm}=\sqrt{\frac{(2q+2n+1)}{4\pi}\frac{(q+n-m)!(q+n+m)!}{n!(2q+n)!}} \tag{5}$$

and

$$J_j=\prod_k{}'(u_jv_k-v_ju_k)\exp\left(\frac{i}{2}(\phi_j+\phi_k)\right). \tag{6}$$

The prime over the product symbol signifies $k\neq j$. We stress that the subscript n in $Y^{CF}_{qnm}(\Omega_j)$ refers to the CF-LL index; the wave function is strictly within the lowest *electronic* LL for arbitrary n. The derivation of the form given in Eq. (4) is given explicitly in Ref. 26 from which we only have quoted the final result.

It is noted that in the spherical geometry the degeneracy in successive CF LL's is not equal; therefore the filling factor of a state is taken to be its value in the thermodynamic limit ($\nu=\lim_{N\to\infty}2Q/N$).

With the explicit wave function above, the ground-state Coulomb energy per particle is calculated according to

$$E = \frac{1}{N}\frac{\langle\Psi|V|\Psi\rangle}{\langle\Psi|\Psi\rangle}, \tag{7}$$

$$V = \sum_{i<j}\frac{e^2}{\epsilon R_{ij}}, \tag{8}$$

where ϵ is the background dielectric constant,

$$R_{ij} = 2R\left|\cos\frac{\theta_i}{2}\sin\frac{\theta_j}{2} - \cos\frac{\theta_j}{2}\sin\frac{\theta_i}{2}e^{i(\phi_i-\phi_j)}\right| \tag{9}$$

is the cord distance between two electrons located on the sphere at Ω_i and Ω_j, and $R=\sqrt{Q}$ is the radius of the sphere in units of magnetic length, $l\equiv\sqrt{\hbar c/eB}$.

Comparisons[26–28] of the ground-state energy obtained using the noninteracting CF wave function $\Psi^{(0)}$ with values from exact diagonalization have shown an accuracy of $\sim 0.2\%$. This is remarkable considering the fact that the CF wave function is a trial wave function with no adjustable parameters. Furthermore, according to the variational theorem, it provides a strict upper bound to the energy.

III. EXPANDED COMPOSITE FERMION BASIS

Composite fermions are indeed very weakly interacting, as is evident by the accuracy of $\Psi^{(0)}$. To obtain a more accurate excitation spectrum, we incorporate into theory the residual interactions among composite fermions perturbatively. The effect of the residual interactions is to cause a hybridization with higher CF LL's, which modifies $\Psi^{(0)}$ and the ground-state energy, as studied in Ref. 16.

To obtain the quantitative effects of CF-LL mixing, we diagonalize the Coulomb Hamiltonian, for each value of angular momentum,[29] in an extended basis space,

$$[\{\Psi^{(0)}\},\{\Psi_\beta^{(1)}\},\{\Psi_\gamma^{(2)}\},\ldots,\{\Psi_\eta^{(J)}\}]. \tag{10}$$

Here, $\Psi_\mu^{(j)}=\Phi_\mu^{CF(j)}$ denote states in which j composite fermions have been excited from the highest occupied CF LL to the lowest unoccupied CF LL, with μ labeling all CF particle-hole configurations in that subspace.[30] The composite fermion excited state $\Psi_\mu^{(j)}$ corresponding to a definite value of L is in general a superposition of Slater determinants. We assume, with no loss of generality, that the z component of the total orbital angular momentum L_z of the excited state is zero.

The basis states are depicted schematically in Fig. 1. In the $J=0$ sector the basis is $\{\Psi^{(0)}\}$ containing only one state, the state with n CF LL's completely occupied; this is the ground state in the approximation in which the interaction between the composite fermions is neglected. It is a uniform state with angular momentum $L=0$, shown schematically in Fig. 1(a). For filling factors of the form $\nu=1/(2p+1)$, $\Psi^{(0)}$ is identical to Laughlin's wave function.[31]

Panels (a) and (b) in Fig. 1 show the $J=1$ basis $[\{\Psi^{(0)}\},\{\Psi_\beta^{(1)}\}]$, which includes the uniform ground state described above as well as the lowest branch of neutral excitation. Simple counting shows that the latter has one state for each value of angular momentum $L=2,\ldots\tilde{N}$, where $\tilde{N}$ is the number of composite fermions in the topmost filled CF LL. This basis gives the excitation spectrum studied previously, for example in Ref. 18.

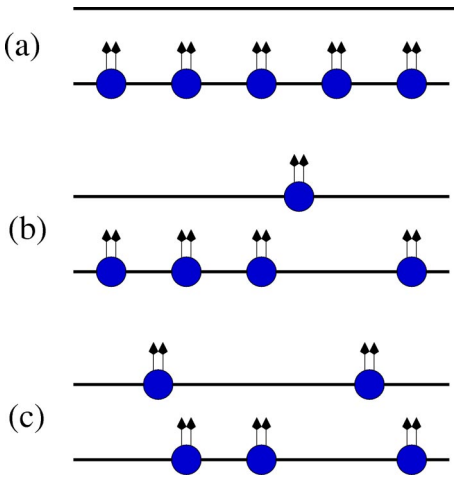

FIG. 1. Schematic depiction of the physical picture of the excitations of a FQHE state in terms of composite fermions. A dot represents an electron and an arrow represents a quantized vortex (or magnetic-flux quantum). A ^{2p}CF is depicted as a dot with $2p$ arrows emanating from it. The horizontal lines are representative of kinetic energy levels of composite fermions. Panel (a) shows the one filled Landau level state of ^{2}CFs. Panels (b) and (c) show excitations containing one and two CF excitons, respectively.

Together, all three panels of Fig. 1 show the $J=2$ composite-fermion basis. The basis for $J\geqslant 2$ is more complicated. In general, there now is more than one basis function in each angular momentum sector. Effectively, we are expanding the low-energy basis space to include the effects of CF-LL mixing, which should produce a quantitatively more accurate description of the excitation spectrum than Ref. 18.

The basis thus obtained is in general not orthogonal. An orthonormal basis is constructed through the standard Gram-Schmidt (GS) procedure, which we implement numerically. Let us relabel the basis of Eq. (10) for a given L as $[\chi_1,\chi_2,\ldots,\chi_\delta]$. Using Monte Carlo methods (Metropolis algorithm) we numerically calculate the inner products $\langle\chi_i|\chi_j\rangle$ and Coulomb matrix elements $\langle\chi_i|V|\chi_j\rangle$. Because the Monte Carlo is most efficient when the quantity being evaluated is positive definite,[32] we use the following expressions:

$$\langle\chi_i|\chi_j\rangle = \frac{\langle\chi_i+\chi_j|\chi_i+\chi_j\rangle - \langle\chi_i|\chi_i\rangle - \langle\chi_j|\chi_j\rangle}{2} \tag{11}$$

and

$$\langle\chi_i|V|\chi_j\rangle = \frac{\langle\chi_i+\chi_j|V|\chi_i+\chi_j\rangle - \langle\chi_i|V|\chi_i\rangle - \langle\chi_j|V|\chi_j\rangle}{2}. \tag{12}$$

To calculate the above quantities, ~ 10 Monte Carlo runs were performed with $\sim 10^6$ iterations each.

The new orthonormal basis is defined as $[\varphi_1,\varphi_2,\varphi_3,\ldots\varphi_{\delta'}]$ where δ' is the number of orthonormal basis states, which is in general less than or equal to δ.

According to the GS procedure we set $\varphi_1=\chi_1$ and compute φ_2, φ_3, $\ldots$, $\varphi_{\delta'}$, iteratively according to

$$\varphi_i=\chi_i-\frac{\langle\chi_i|\chi_1\rangle}{\langle\chi_1|\chi_1\rangle}\chi_1-\frac{\langle\chi_i|\varphi_2\rangle}{\langle\varphi_2|\varphi_2\rangle}\varphi_2-\ldots$$
$$-\frac{\langle\chi_i|\varphi_{i-1}\rangle}{\langle\varphi_{i-1}|\varphi_{i-1}\rangle}\varphi_{i-1}. \quad (13)$$

All of the φ_i can be written in terms of the original basis along with their overlap matrix elements calculated from Monte Carlo.

If $\delta'<\delta$ then the original basis is linearly dependent. The Gram-Schmidt procedure will make this evident; φ_i will equal zero if it is linearly dependent on the previous φ_j. To insure that our calculation captures all of the linearly independent basis states, we find it useful to start with a random superposition of the original basis functions.

The Coulomb matrix elements $\langle\varphi_i|V|\varphi_j\rangle$ can be expressed in terms of the Coulomb matrix elements computed from the original basis, namely $\langle\chi_i|V|\chi_j\rangle$. After calculating the Coulomb matrix elements in the new orthogonal basis, the matrix is diagonalized, obtaining eigenstates $\chi^{(J)}$ along with their corresponding eigenenergies $E^{(J)}$. This procedure is implemented for each angular momentum L separately.

To give an idea of the size of the full Hilbert space compared to the low-energy basis space we work with, consider $N=10$ electrons at $2Q=117$ ($\nu=1/13$). In terms of electrons, this system has a Hilbert space with dimension $\sim 8.9\times 10^{13}$, making any exact calculations impossible. In contrast, in terms of composite fermions, truncating at $J=2$, the basis has only 172 linearly independent states. Further, while the full electron Hilbert space grows exponentially as the filling factor decreases, for composite fermions the dimension of the low-energy basis for a given J does not depend on filling factor, allowing an investigation of arbitrary small values of ν.

Of course, if we keep increasing J, the dimension of the low-energy basis space will grow until we obtain, in principle, the exact spectrum (although that would not be the most efficient method to calculate the exact spectrum). The point here is that the CF theory enables us to directly zoom into the low-energy part of the Hilbert space, thereby producing an extremely accurate estimation of the low-energy spectrum with relatively few basis states.

IV. COMPARISON WITH EXACT RESULTS

It was shown in Ref. 16 that the inclusion of CF-LL mixing leads to an improved ground-state energy. To test the validity of the method for excited states, we first compare our results with the excitation spectra of one of the largest systems ($N=10, 2Q=27$) for which exact results are known. The dimension of the full Hilbert space in the $L_z=0$ subspace is 246 448, whereas the corresponding dimension of the orthogonal CF basis used in our study (with $J=2$) is 172, as mentioned above, with the largest matrix diagonalized being 18×18.

Figure 2 shows a plot of energy as a function of angular momentum for this system ($N=10$, $2Q=27$) computed from exact diagonalization, and also from the CF theory at two levels of approximation. The dashes and dots in Fig. 2(a) represent E^{exact} and $E^{(1)}$, respectively.[33] The Monte Carlo uncertainty in the energy is not shown when it is smaller than the symbol size. The energy is given in units of $e^2/\epsilon l$ where $l=\sqrt{\hbar c/eB}$ is the magnetic length. All energies include interaction with a uniform positive background, and have been corrected for finite-size deviation in the electron density from the thermodynamic limit by multiplication of $\sqrt{\rho/\rho_N}=\sqrt{2Q\nu/N}$, where ρ and ρ_N are the densities in the thermodynamic limit and for the N particle system, respectively. We see that $E^{(1)}$ describes the lowest band of excitations qualitatively, and has a quantitative accuracy of better than 0.3%. Notice that there is no $L=1$ state present in $E^{(1)}$; The $L=1$ state of the electron system at $2q=9$ is annihilated[34] by the lowest LL projection operator P_{LLL}.

For the next level of approximation we consider the basis corresponding to $J=2$. Figure 2(b) shows E^{exact} and $E^{(2)}$ as a function of angular momentum. The lowest energy at each L is now much closer to the exact result, the two often being indistinguishable within the Monte Carlo uncertainty (Table I). Even though our present interest is with the lowest energy

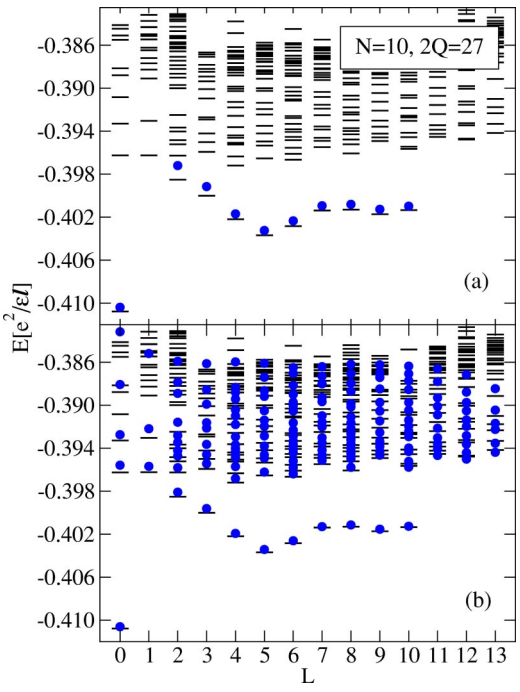

FIG. 2. The energy spectrum as a function of L for a system at $\nu=1/3$ with $N=10$ particles at flux value $2Q=27$. The energy per particle is reported in this and subsequent figures in units of $e^2/\epsilon l$ where $l\equiv\sqrt{\hbar c/eB}$ is the magnetic length and ϵ is the dielectric constant of the host semiconductor. The black dashes are energies obtained by exact diagonalization and the dots are $E^{(1)}$ (earlier reported in Ref. 33) and $E^{(2)}$ in panels (a) and (b), respectively. The Monte Carlo error is smaller than the symbol size. The finite-size change in the electron density from its thermodynamic value has been incorporated by multiplying each energy by $\sqrt{\rho/\rho_N}=\sqrt{2Q\nu/N}$.

TABLE I. The second column gives the exact energy per particle for the lowest energy at orbital angular momenta $L=0,1,\ldots 10$ for ten particles at $2Q=27$ ($\nu=1/3$). $E^{(1)}$ is the energy per particle of the state with a single-particle hole pair of composite fermions. $E^{(2)}$ is the energy per particle after the CF Landau level mixing is incorporated, through diagonalization in the Fock space of all states containing 0, 1, or 2 pairs of particle hole excitations of composite fermions, as described in the text. The last column gives the percent error for cases where $E^{(2)}$ differs from E^{exact} significantly. The Monte Carlo uncertainty in the last digit is shown in parentheses.

L	E^{exact}	$E^{(1)}$	$E^{(2)}$	Error (%)
0	−0.410 628 97	−0.410 39(2)	−0.410 62(3)	
1	−0.396 090 58		−0.395 7 (1)	0.1
2	−0.398 368 47	−0.397 2 (1)	−0.398 1 (1)	0.07
3	−0.399 854 58	−0.399 16 (8)	−0.399 6 (1)	0.06
4	−0.402 038 92	−0.401 7 (1)	−0.401 94 (5)	0.02
5	−0.403 540 97	−0.403 24 (8)	−0.403 43 (4)	0.03
6	−0.402 684 31	−0.402 3 (1)	−0.402 61 (5)	0.02
7	−0.401 235 1	−0.400 94 (8)	−0.401 3 (2)	
8	−0.401 153 14	−0.400 81 (6)	−0.401 15 (5)	
9	−0.401 578 15	−0.401 27 (5)	−0.401 5 (1)	
10	−0.401 203 51	−0.400 98 (8)	−0.401 3 (1)	

excitations, we note that we also get a reasonably accurate description of higher energy excitations as well as the excitations at values of L not available for $J=1$ (for example, $L=1$ and $L>\tilde{N}$). Given the quantitative accuracy of the low-energy spectrum, we restrict our study to $J=2$.

Such an accurate description of the excitation spectrum of the FQHE state gives yet another compelling theoretical justification for the CF theory, and for the remarkably simple physical picture for the excitations in terms of composite fermions, shown in Fig. 1.

V. NEUTRAL EXCITATIONS AT SMALL ν

A. $\nu=1/9$ revisited

Having ascertained the validity of our method, we proceed to calculate the low-energy spectra for small ν. As was mentioned above, an instability in the excitation spectrum was seen for $\nu\leqslant 1/9$ using $E^{(1)}$. However, $E^{(2)}$ is a more accurate description of this spectrum which we now investigate.

Here we calculate the CF exciton energy $\Delta^{ex}(k)$, the energy required to create a CF particle-hole pair out of the ground state, for $J=1$ and $J=2$, as a function of wave vector $k\equiv L/R=L/\sqrt{Q}$. The ground state for $J=1$ is the noninteracting CF state, while the ground state for $J=2$ is the more accurate weakly interacting CF ground state with energy $E^{(2)}(0)$. Figure 3 shows $\Delta^{ex}(k)$ for $J=1$ in panel (a) and $J=2$ in panel (b) for $\nu=1/9$. The different symbols represent different system sizes and convergence to the thermodynamic limit is evident by the fact that the energies for different N fall on a single curve. In this and all subsequent figures, only the lowest excitation energy is shown at each wave vector (for each N).

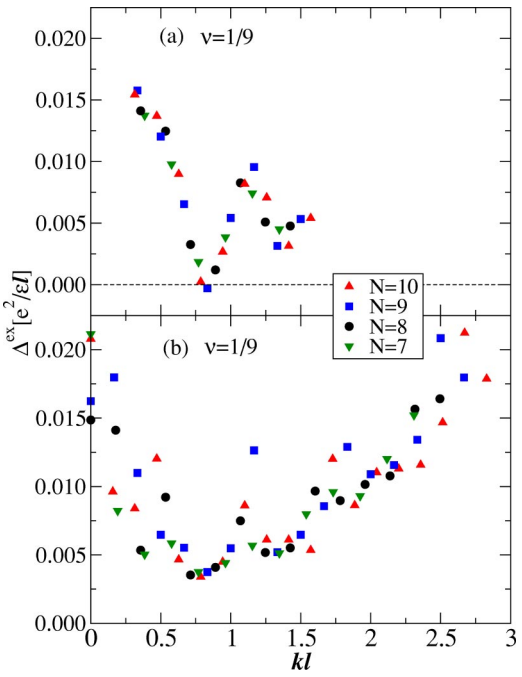

FIG. 3. The exciton energy Δ^{ex} as a function of $k=L/\sqrt{Q}$ at $\nu=1/9$. Different symbols represent Δ^{ex} for different system sizes N. Panel (a) is from Ref. 18 and shows $E^{(1)}(k)$. An instability is seen for a wave vector value that is close to the reciprocal-lattice vector of the Wigner crystal. Panel (b) is the more accurate spectrum $E^{(2)}(k)$. No instability is seen in (b); there exists a finite energy gap for all values of k.

At the simplest level of approximation [Fig. 3(a)] we recover the instability in the spectrum for a value of the wave vector $kl\sim 0.85$, which was earlier interpreted[18] as indicating a collapse of the FQHE for $\nu\leqslant 1/9$. For $E^{(2)}$, however, a finite excitation gap exists for all values of k and the instability disappears. The slightly more accurate energy spectrum of the CF liquid at $\nu=1/9$ thus leads to a *qualitatively* different conclusion. The lack of instability is consistent with Ref. 16 where it was shown that the CF liquid state very likely has lower energy than the WC state for $\nu=1/9$.

Of course, each $E^{(2)}$ is lower than the corresponding $E^{(1)}$, but the energy difference Δ^{ex} can either increase or decrease. Figure 3 shows that the ground-state energy decreases more than the energy of the exciton. For the $N=10$ particle system, for example, the ground-state energy (per particle) has gone from $-0.249\,133(20)e^2/\epsilon l$ in Fig. 3(a) to $-0.249\,788(10)e^2/\epsilon l$ in Fig. 3(b). It is also important to note that the dimension for the CF basis for the CF exciton at its minimum is, in general, larger than that for the $L=0$ ground state, giving the former more variational freedom. (For example, for Fig. 2, the number of basis states at $L=5$ is 13, which ought to be compared to five basis states at $L=0$.) As a result, one might have *a priori* expected the $L=0$ ground state to be less affected by an admixture with higher CF LL's than the CF exciton at its minimum. Our result is exactly the opposite, which makes it all the more convincing.

For $J=2$, we show the lowest energy for a more extended range of L than available for $J=1$. For $J=1$, the large L

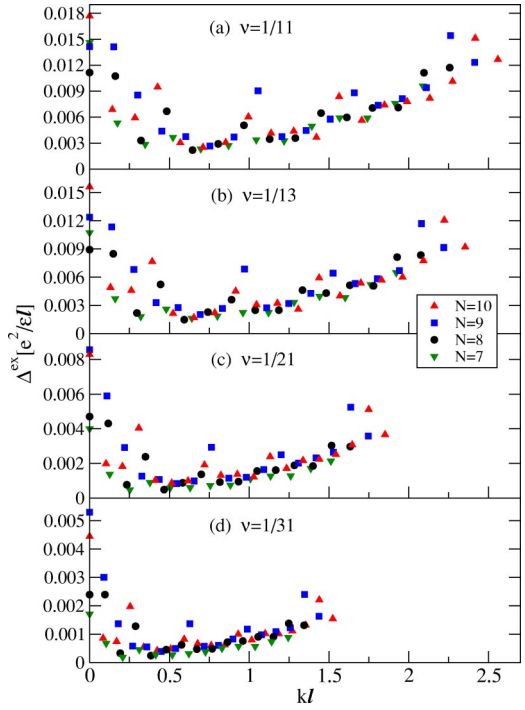

FIG. 4. The exciton energy Δ^{ex} as a function of k (for $J=2$) for several values of N at fillings of the form $\nu=1/(2p+1)$. Different symbols represent different system sizes. Panels (a), (b), (c), and (d) show the results for $\nu=1/11,1/13,1/21$, and $1/31$, respectively. There exists a finite energy gap for all values of k in (a)–(d) indicating that the CF liquid is stable to excitations at these filling factors.

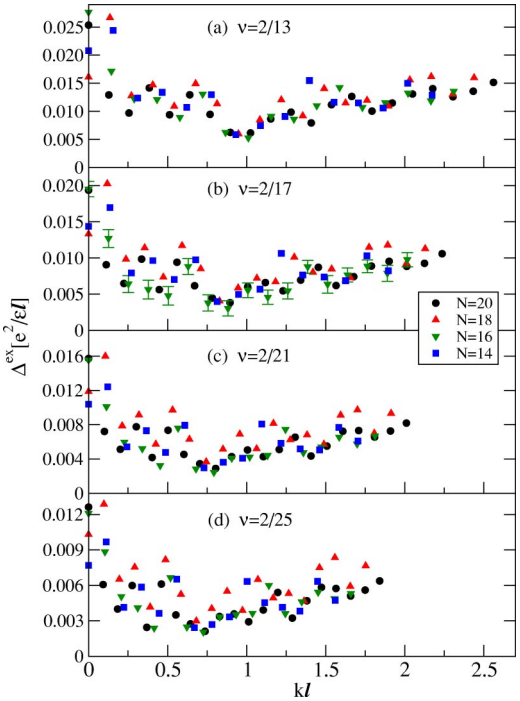

FIG. 5. The exciton energy Δ^{ex} as a function of k (for $J=2$) for several values of N at fillings of the form $\nu=2/(4p+1)$. Different symbols represent different system sizes. Panels (a), (b), (c), and (d) show results for $\nu=2/13,2/17,2/21$, and $2/25$, respectively. There is a finite energy gap for all values of k in (a)–(d) indicating that the CF liquid is stable to excitations at these filling factors.

limit of the exciton branch is a far separated particle-hole pair of composite fermions, which gives the gap relevant to transport experiments. Care must be exercised *not* to interpret the energy at large L for the $J=2$ results shown in this paper as the transport gap. (The transport gap, which is the energy required to create a *single* far separated pair of CF particle and CF hole, is the large L limit of the $J=1$ excitation branch. In Fig. 2, this would be the energy of the excited state at $L=10$. The energy is somewhat affected by CF level mixing, as in going from Fig. 2(a) to (b), but is distinct from the energy of the largest L excitation in the $J=2$ sector of Fig. 3.)

B. Excitations at very low filling factors

In this subsection we investigate where an instability in the exciton state may occur by going to yet smaller filling factors. We have computed the spectra from $E^{(2)}$ for filling factors $\nu=2/13,2/17,2/21,1/11,2/25,1/13,1/21$, and $1/31$. The lowest energies at each wave vector are displayed in Figs. 4 and 5.

From Fig. 4(d) we see that even down to the smallest filling factor investigated, $\nu=1/31$, the energy gap remains positive. The excitation minima located near $k_{WC}l$ (where $k_{WC}l$ is the reciprocal-lattice vector of the WC) seem to have approached a well defined thermodynamic limit. Finite-size effects are more severe close to $kl=0$, as expected, but the energies are too high there to cause instability.

The states investigated in Fig. 5 correspond to two CF LL's filled up by ^{6}CF's, ^{8}CF's, ^{10}CF's, and ^{12}CF's, respectively. Here, we have the choice of exciting composite fermions from either of the two filled CF LL's. Because our objective is simply to create an extended basis to provide some variational freedom at low energies, we only promote j composite fermions from the topmost CF LL; we believe that this should be sufficient for our purpose.[30]

In Fig. 5, the lowest excitation energies at $\nu=2/17,2/21$, and $2/25$, which have the form $\nu=2/(4p+1)$, do not fall on a single curve, which is indicative of significant finite-size effects at these fractions for the values of N considered. An investigation of larger N would be required for an accurate estimation of the gap, but we have not pursued that here because of a lack of urgent experimental motivation. It is sufficient to note for now that the gap remains positive for all cases studied.

VI. FILLING FACTOR DEPENDENCE

Will there be a transition, in our theory, into a Wigner crystal state as we go to still lower filling factors? To look into that question, we study how the minimum energy, labeled Δ^{ex}_{min}, behaves as a function of the filling factor. The general trend expected is that Δ^{ex}_{min} will decrease with decreasing ν, perhaps becoming zero at some filling, signaling an instability of the CF liquid state.

The most effective way to answer this question is by considering the value of the minimum-energy gap in the thermo-

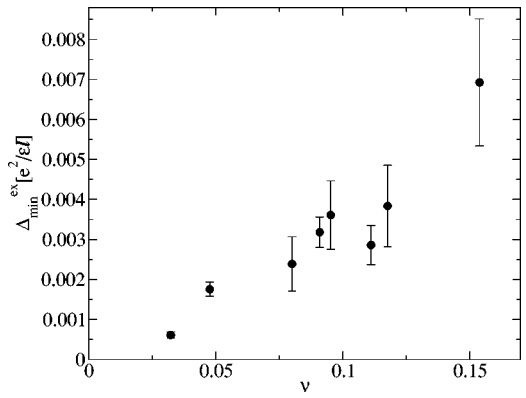

FIG. 6. The thermodynamic limit of the minimum exciton energy Δ^{ex}_{min} as a function of ν. Δ^{ex}_{min} is reduced with decreasing filling factor, but remains positive down to the smallest value of filling factor studied. The uncertainty, indicated by error bars, is mainly from the thermodynamic extrapolation.

dynamic limit ($N\to\infty$). In order to determine Δ^{ex}_{min} at the thermodynamic limit we take, for each ν, the lowest energy excitation for each system size N and perform a linear extrapolation in N^{-1} using standard techniques. For $\nu=1/9$, 1/11, 1/21, and 1/31 we consider $N=7$, 8, 9, and 10, whereas for $\nu=2/13$, 2/17, 2/21, and 2/25 we consider $N=14$, 16, 18, and 20.

Figure 6 displays the thermodynamic limit of Δ^{ex}_{min} as a function of filling factor ν. As expected, Δ^{ex}_{min} decreases with decreasing ν. However, it is not possible to reach a definite conclusion regarding where Δ^{ex}_{min} will hit zero. Our results do not rule out the possibility that it remains finite (for our model) to arbitrarily small ν.

VII. FINITE THICKNESS

So far, we have taken the electron system to be strictly two dimensional and neglected the electronic LL mixing. The latter ought to be a good approximation, given the large fields needed to reach the low filling factors in question for typical densities. In this section we take account of the former by considering the finite extent of the electronic wave function in the direction perpendicular to the two-dimensional plane (z direction). The quantitative effect of finite width is important to ascertain because some of the experiments of Pan *et al.*[15] are performed in fairly wide quantum wells. We have focused on $\nu=1/9$ and 2/17. The neutral excitation energies are, of course, calculated using the energies $E^{(2)}$.

It is well known that the general effect of the inclusion of finite thickness effects is a softening of the short distance part of the repulsive interaction, which causes a lowering of all of the energies. The finite thickness effects will be incorporated into our calculation by considering an effective interaction obtained through a self-consistent local-density approximation (LDA) calculation, following Refs. 35 and 36. As an example, we will only consider the square quantum well confinement potential, with widths in the range of 0–60 nm and electron densities from $\rho=3.0\times10^{10}$ to 5.0×10^{11} cm^{-2}.

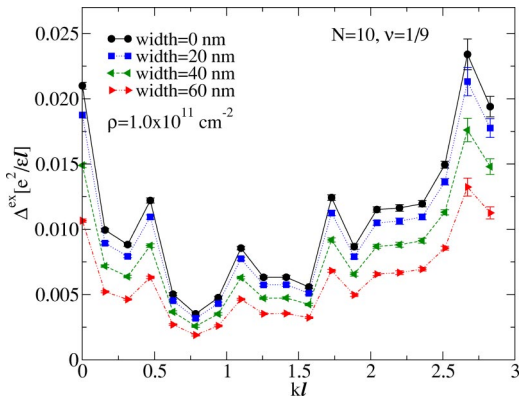

FIG. 7. Δ^{ex} as a function of kl for $N=10$ particles at $\nu=1/9$. All four curves correspond to an electron density of $\rho=1.0\times10^{11}$ cm^{-2} with square-well potential widths of 0, 20, 40, and 60 nm.

Figures 7–10 show the lowest energy excitations for $\nu=1/9$ and 2/17 for system sizes of $N=10$ and 20, respectively, for various widths and electron densities. The first two show the width dependence for square quantum well widths of 0, 20, 40, and 60 nm for a fixed density of $\rho=1.0\times10^{11}$ cm^{-2}. The energy of the CF exciton is reduced at all wave vectors with increasing width, as expected. The last two show the density dependence for a fixed width of 30 nm.

The effect of finite thickness seems rather simple. The shape of the dispersion is not affected by thickness, only the magnitude. In fact, the exciton energies for finite thickness can be obtained, to a good approximation, from those at zero thickness by scaling the entire dispersion by a thickness-dependent (but wave-vector-independent) factor. For the two filling factors ($\nu=1/9$ and 2/17) considered, this multiplicative factor also appears to be filling factor independent, but we have not confirmed that over a wider range of fillings.

The main point here is that, within the present level of approximation, no instability occurs at $\nu=1/9$ or 2/17 as a function of thickness. We expect that to be the case also at larger filling factors, in the width and density ranges considered.

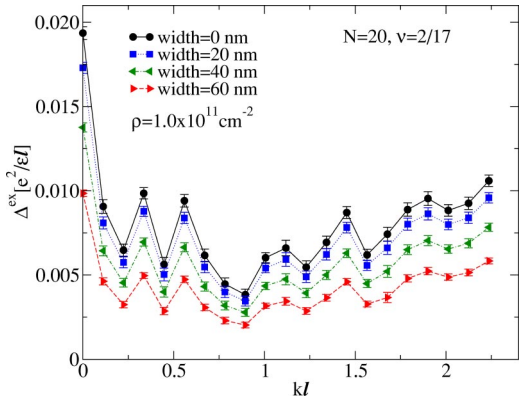

FIG. 8. Δ^{ex} as a function of kl for $N=20$ particles at $\nu=2/17$. All four curves correspond to an electron density of $\rho=1.0\times10^{11}$ cm^{-2} with square-well potential widths of 0, 20, 40, and 60 nm.

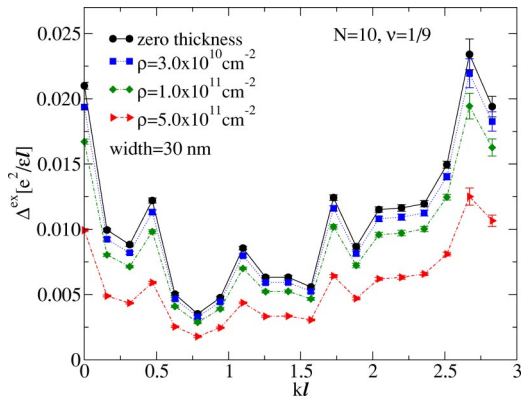

FIG. 9. Δ^{ex} as a function of kl for $N=10$ particles at $\nu=1/9$. All four curves correspond to a square-well potential width of 30 nm with electron densities of $\rho=3.0\times10^{10}$, 1.0×10^{11}, and 5.0×10^{11} cm^{-2}.

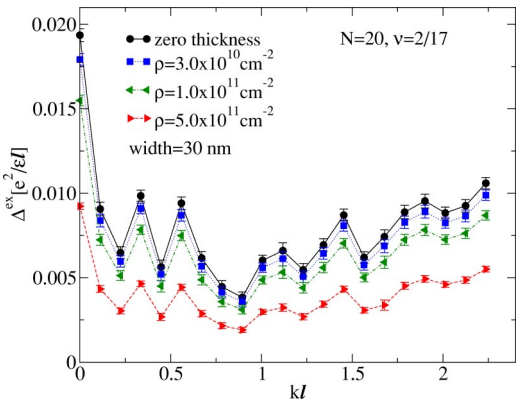

FIG. 10. Δ^{ex} as a function of kl for $N=20$ particles at $\nu=2/17$. All four curves correspond to a square-well potential width of 30 nm with electron densities of $\rho=3.0\times10^{10}$, 1.0×10^{11}, and 5.0×10^{11} cm^{-2}.

In the experiment of Ref. 15, the 1/9 state was observed for a density of $\rho=1.0\times10^{11}$ cm^{-2} for a quantum well of width 50 nm. The minimum excitation energy here is approximately $0.0025e^2/\epsilon l$, which, for a magnetic field of $B\approx40$ T, is equal to ~800 mK. For $\nu=1/7$, the minimum energy is $\sim0.004e^2/\epsilon l$, which, after taking into account finite thickness corrections, gives an energy of ~700 mK at $B=29$ T. These numbers ought to be compared to the experimental temperatures of 200–300 mK above which FQHE at these fillings is not seen.[15] As usual, the experimental energy scales are smaller than those obtained from theory, with the discrepancy attributable to theory's neglect of disorder.

VIII. CONCLUSION

An instability of the FQHE found earlier for $\nu=1/9$ is eliminated when the CF theory is improved to take into account CF-LL mixing, caused by the weak residual interaction between composite fermions. The lack of instability persists down to $\nu=1/31$, the smallest filling factor studied. While a first-order transition into a Wigner crystal state cannot be ruled out from our study, it indicates that the liquid state of composite fermions may be robust down to much smaller fillings than earlier believed.

ACKNOWLEDGMENTS

This work was supported in part by the National Science Foundation under Grant Nos. DGE-9987589 (IGERT) and DMR-0240458. We are grateful to the High Performance Computing (HPC) Group led by V. Agarwala, J. Holmes, and J. Nucciarone at the Penn State University ASET (Academic Services and Emerging Technologies) for assistance and computing time with the LION-XL cluster.

[1] D.C. Tsui, H.L. Stormer, and A.C. Gossard, Phys. Rev. Lett. **48**, 1559 (1982).
[2] *Perspectives in Quantum Hall Effects*, edited by S. Das Sarma and A. Pinczuk (Wiley, New York, 1997).
[3] *Composite Fermions*, edited by Olle Heinonen (World Scientific, New York, 1998).
[4] E.P. Wigner, Phys. Rev. **46**, 1002 (1934).
[5] P.K. Lam and S.M. Girvin, Phys. Rev. B **30**, 473 (1984).
[6] K. Esfarjani and S.T. Chui, Phys. Rev. B **42**, 10 758 (1990).
[7] X. Zhu and S.G. Louie, Phys. Rev. B **52**, 5863 (1995).
[8] Kun Yang, F.D.M. Haldane, and E.H. Rezayi, Phys. Rev. B **64**, 081301 (2001).
[9] H.W. Jiang, R.L. Willett, H.L. Stormer, D.C. Tsui, L.N. Pfeiffer, and K.W. West, Phys. Rev. Lett. **65**, 633 (1990).
[10] V.J. Goldman, M. Santos, M. Shayegan, and J.E. Cunningham, Phys. Rev. Lett. **65**, 2189 (1990).
[11] M. Shayegan, *Perspectives in Quantum Hall Effects* (Ref. 2), pp. 343–384.
[12] V.J. Goldman, M. Shayegan, and D.C. Tsui, Phys. Rev. Lett. **61**, 881 (1988).
[13] J.R. Mallett, R.G. Clark, R.J. Nicholas, R. Willett, J.J. Harris, and C.T. Foxon, Phys. Rev. B **38**, 2200 (1988).
[14] H. Buhmann, W. Joss, K. v. Klitzing, I.V. Kukushkin, A.S. Plaut, G. Martinez, K. Ploog, and V.B. Timofeev, Phys. Rev. Lett. **65**, 1056 (1990).
[15] W. Pan, H.L. Stormer, D.C. Tsui, L.N. Pfeiffer, K.W. Baldwin, and K.W. West, Phys. Rev. Lett. **88**, 176802 (2002).
[16] S.S. Mandal, M.R. Peterson, and J.K. Jain, Phys. Rev. Lett. **90**, 106403 (2003).
[17] J.K. Jain, Phys. Rev. Lett. **63**, 199 (1989).
[18] R.K. Kamilla and J.K. Jain, Phys. Rev. B **55**, R13417 (1997).
[19] A. Pinczuk, B.S. Dennis, L.N. Pfeiffer, and K. West, Phys. Rev. Lett. **70**, 3983 (1993); Physica B **249B-251B**, 40 (1998).
[20] M. Kang, A. Pinczuk, B.S. Dennis, L.N. Pfeiffer, and K.W. West, Phys. Rev. Lett. **86**, 2637 (2001).
[21] I. Dujovne, A. Pinczuk, M. Kang, B.S. Dennis, L.N. Pfeiffer, and K.W. West, Phys. Rev. Lett. **90**, 036803 (2003); I. Dujovne, C.F. Hirjibehedin, A. Pinczuk, M. Kang, B.S. Dennis, L.N. Pfeiffer, and K.W. Wang, Solid State Commun. **127**, 109 (2003).

[22] H.D.M. Davies, J.C. Harris, J.F. Ryan, and A.J. Turberfield, Phys. Rev. Lett. **78**, 4095 (1997).
[23] C.J. Mellor, R.H. Eyles, J.E. Digby, A.J. Kent, K.A. Benedict, L.J. Challis, M. Henini, C.T. Foxon, and J.J. Harris, Phys. Rev. Lett. **74**, 2339 (1995).
[24] U. Zeitler, A.M. Devitt, J.E. Digby, C.J. Mellor, A.J. Kent, K.A. Benedict, and T. Cheng, Phys. Rev. Lett. **82**, 5333 (1999).
[25] T.T. Wu and C.N. Yang, Nucl. Phys. B **107**, 365 (1976).
[26] J.K. Jain and R.K. Kamilla, Phys. Rev. B **55**, R4895 (1997).
[27] J.K. Jain and R.K. Kamilla, Int. J. Mod. Phys. B **11**, 2621 (1997).
[28] J.K. Jain, C.C. Chang, G.S. Jeon, and M.R. Peterson, Solid State Commun. **127**, 805 (2003).
[29] The interaction commutes with the total angular momentum and therefore does not mix states with different L.
[30] Another natural choice would be to consider all excited states with effective kinetic energy equal to j in units of the CF cyclotron energy, which would in general involve excitations of composite fermions across several CF levels. Defined this way, the dimension of the basis would be significantly larger than the one considered here, making a numerical diagonalization prohibitively time consuming in many cases of interest. As seen in Table I, however, the present enlargement of the basis already produces very accurate energies.
[31] R.B. Laughlin, Phys. Rev. Lett. **50**, 1395 (1983).
[32] S.S. Mandal and J.K. Jain, Phys. Rev. B **66**, 155302 (2002).
[33] J.K. Jain and R.K. Kamilla, *Composite Fermions* (Ref. 3), pp. 1–90.
[34] G. Dev and J.K. Jain, Phys. Rev. Lett. **69**, 2843 (1992).
[35] M.W. Ortalano, S. He, and S. Das Sarma, Phys. Rev. B **55**, 7702 (1997).
[36] K. Park, N. Meskini, and J.K. Jain, J. Phys.: Condens. Matter **11**, 7283 (1999).